

---

## The cosmic ray primary composition in the knee region through the EAS electromagnetic and muon measurements at EAS-TOP

---

S. Valchierotti <sup>1</sup> on behalf of the THE EAS-TOP Collaboration

(1) *Dipartimento di Fisica Generale dell'Univerità, I.N.F.N., Torino, ITALY*

---

### Abstract

The evolution of the cosmic ray primary composition in the energy range  $10^{15} \div 10^{16}$  eV (i.e. the “knee” region) is studied by means of the e.m. and muon data of the Extensive Air Shower EAS-TOP array. The measurement is performed by analyzing the whole distributions of the detected muon numbers vs. the shower size in terms of three mass groups: *light* (p,He), *intermediate* (CNO), and *heavy* (Fe). In the “knee” region the obtained evolution of the energy spectra leads to a steep spectrum of the *light* mass group ( $\gamma_{p,He} > 3.1$ ), a possible break of the *intermediate* one or a spectrum on the average harder than for the *light* mass group ( $\gamma_{CNO} \simeq 2.75$ ), and a constant slope for the spectrum of the *heavy* primaries ( $\gamma_{Fe} \simeq 2.3 \div 2.7$ ) consistent with the direct measurements. With increasing energy, the average primary mass changes from  $\langle \ln A \rangle = 1.6 \div 1.9$  at  $E_0 \simeq 1.5 \cdot 10^{15}$  eV to  $\langle \ln A \rangle = 2.8 \div 3.1$  at  $E_0 \simeq 1 \cdot 10^{16}$  eV. The result supports the standard acceleration and propagation models of galactic cosmic rays that predict rigidity dependent cut-offs for the primary spectra of the different nuclei.

### 1. The detectors

The EAS-TOP array was located at Campo Imperatore, National Gran Sasso Laboratories, 2005 m a.s.l., 820 g·cm<sup>-2</sup> atmospheric depth. The e.m. detector consisted of 35 modules 10 m<sup>2</sup> each of plastic scintillators distributed over an area of 10<sup>5</sup> m<sup>2</sup> [1]. Events with at least six nearby modules fired, and the largest number of particles recorded by a module internal to the edges of the array are selected. The core location ( $X_c, Y_c$ ), the e.m. shower size  $N_e$  and the slope of the lateral distribution function ( $s$  parameter) are obtained fitting the recorded number of particles in each module, with resolutions  $\sigma_{N_e}/N_e \simeq 0.1$ ;  $\sigma_{X_c} = \sigma_{Y_c} \simeq 5$  m;  $\sigma_s \simeq 0.1$ . The arrival direction of the shower is measured from the times of flight among the modules with resolution  $\sigma_\theta \simeq 0.9^\circ$ .

The muon-hadron detector [2] for the present analysis is used as a tracking module of 9 active planes. Each plane includes two layers of streamer tubes (12 m length, 3 × 3 cm<sup>2</sup> section) for muon tracking, one layer of proportional tubes for hadron calorimetry, 8 cm of air and 13 cm of iron shield. The total height of the

detector is 280 cm and the surface is  $12 \times 12 \text{ m}^2$ .

## 2. Analysis and results

The analysis of a set of data collected in 8600 hours of data taking is presented in the following; runs without presence of snow at the site have been selected. Events with zenith angle of the e.m. shower  $\theta \leq 17.7^\circ$  are used.

The evolution of the abundances of the different components vs  $N_e$  has been studied by fitting the  $N_{\mu_{180}}$  distributions, where  $N_{\mu_{180}}$  is the number of muons observed in the tracking detector in events with core distances between 180 and 210 m. Events are selected in ranges of shower sizes  $\Delta \text{Log}N_e = 0.2$  from  $\text{Log}N_e = 5.2$  up to  $\text{Log}N_e = 6.6$ , i.e. around the knee position. The intrinsic resolution of the measurement allow fits with three mass groups: *light*, *intermediate* and *heavy* [3]. The three mass groups are represented respectively through p, N and Fe primaries. In order to evaluate the influence of the choice of the mass groups components on the final result, and the systematic effects due to such choice, a second analysis has been performed, in which the *light* mass group is represented through a mixture of 50% proton and 50% helium, while the *intermediate* and the *heavy* ones are still represented by nitrogen and iron (the two analysis will be denoted respectively as ‘p’ and ‘p+He’ in the plots). The relative abundances of the three mass groups in each bin of  $N_e$  are thus obtained directly from the fit of the experimental  $N_{\mu_{180}}$  distributions with the simulated ones. The simulations are based on the QGSJET model [4] as implemented in the CORSIKA code [5]. The total number of simulated events is comparable with the experimental one.

| $\text{Log}N_e$ | 5.2-5.4         | 5.4-5.6         | 5.6-5.8         | 5.8-6.0         | 6.0-6.2         | 6.2-6.4         | 6.4-6.6         |
|-----------------|-----------------|-----------------|-----------------|-----------------|-----------------|-----------------|-----------------|
| $\alpha_p$      | $0.62 \pm 0.01$ | $0.62 \pm 0.02$ | $0.56 \pm 0.02$ | $0.44 \pm 0.02$ | $0.34 \pm 0.02$ | $0.26 \pm 0.03$ | $0.18 \pm 0.04$ |
| $\alpha_N$      | $0.34 \pm 0.02$ | $0.33 \pm 0.03$ | $0.37 \pm 0.02$ | $0.49 \pm 0.02$ | $0.60 \pm 0.04$ | $0.56 \pm 0.05$ | $0.65 \pm 0.07$ |
| $\alpha_{Fe}$   | $0.04 \pm 0.01$ | $0.50 \pm 0.01$ | $0.07 \pm 0.01$ | $0.06 \pm 0.01$ | $0.07 \pm 0.02$ | $0.19 \pm 0.02$ | $0.23 \pm 0.04$ |
| $\chi^2$        | 1.6             | 3.8             | 2.4             | 1.2             | 1.4             | 1.2             | 1.2             |
| $\alpha_{p+He}$ | $0.83 \pm 0.03$ | $0.84 \pm 0.05$ | $0.76 \pm 0.04$ | $0.6 \pm 0.03$  | $0.46 \pm 0.02$ | $0.37 \pm 0.03$ | $0.24 \pm 0.05$ |
| $\alpha_N$      | $0.10 \pm 0.04$ | $0.06 \pm 0.07$ | $0.14 \pm 0.06$ | $0.30 \pm 0.04$ | $0.45 \pm 0.03$ | $0.43 \pm 0.05$ | $0.55 \pm 0.08$ |
| $\alpha_{Fe}$   | $0.08 \pm 0.02$ | $0.11 \pm 0.03$ | $0.10 \pm 0.02$ | $0.10 \pm 0.02$ | $0.09 \pm 0.01$ | $0.21 \pm 0.03$ | $0.26 \pm 0.04$ |
| $\chi^2$        | 5.6             | 8.7             | 7.1             | 2.6             | 0.8             | 1.1             | 1.2             |
| $N$             | 258384          | 120668          | 54492           | 23356           | 10106           | 3890            | 1328            |

**Table 1.** Relative abundances of the three components in seven intervals of  $N_e$  obtained by fitting the  $N_{\mu_{180}}$  distributions and  $\chi^2$  values of the fits.  $N$  is the number of experimental events used in each size interval. The two cases, in which the light mass group is represented by “p” and “50% p + 50% He”, are given.

The results of the analysis are summarized in Tab. 1. The decreasing weight of the *light* elements and the corresponding increase of the *intermediate* and *heavy* ones is observed in both analysis ('p' and 'p+He'), and thus does not depend on the fraction of protons and helium used to describe the *light* mass group. The size spectrum corresponding to each mass group is calculated from such relative abundances, using as normalization the experimental size spectrum. The primary energy distributions of each mass group are obtained by selecting from the whole simulated data the events contributing to such size spectra. The corresponding differential energy spectra are plotted in Fig. 1 together with the extrapolations from the direct measurements [6]. At  $E_0 \sim 10^{15}$  eV the present fluxes and the extrapolated data are in very reasonable agreement, inside the mass groups approximation.

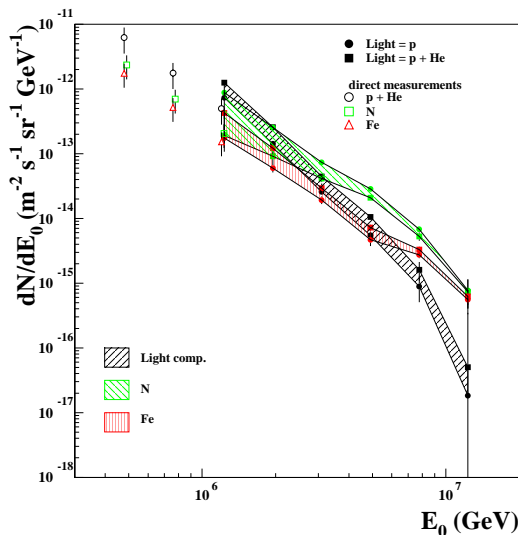


**Fig. 1.** Energy spectra of the three mass groups. To be consistent with the present analysis, in the direct measurements (reported for comparison) the light mass group includes proton and helium primaries.

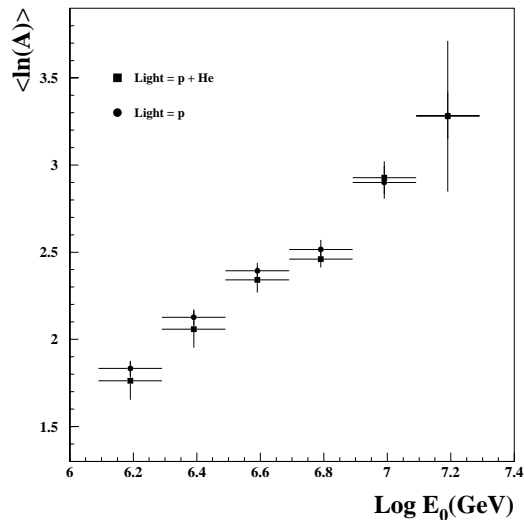


**Fig. 2.** Average value of  $\ln(A)$  vs primary energy  $E_0$ .

The reconstructed spectrum of the *light* mass group results steeper than the one obtained from the direct measurements ( $\gamma_{p,He} > 3.1$ ). A break in the CNO spectrum is possibly observed ( $\gamma_{CNO,1} \simeq 2.5$ ,  $\gamma_{CNO,2} \simeq 3.3$ ) at primary energy  $E_0 \simeq 5 \cdot 10^{15}$  eV, but inside the uncertainties of the assumptions for the light component ('p', or 'p+He') a unique spectral index ( $\gamma_{CNO} \simeq 2.75$ ) is compatible with the data. No steepening is observed in the spectrum of the heavier mass group (iron): the index of the power law spectrum  $\gamma_{Fe} \simeq 2.3 \div 2.7$  fits the data

over the whole energy range and is compatible with the one measured in the TeV range by the direct experiments. We have to remark that even if (due to the mass group approximation and the difficulty in separating protons and helium primaries) the actual breaks in the spectra of the different components cannot really be identified, the increasing steepening of the spectra of the lighter nuclei is independent from the assumptions on the mass group components.

The evolution of  $\langle \ln A \rangle$  vs. primary energy is shown in Fig. 2. Concerning the general behavior, the increasing value of  $\langle \ln A \rangle$  is in accord with the data presented by the KASCADE Collaboration [7], the values of  $\langle \ln A \rangle$  being systematically larger of about 0.5 in the present analysis. The agreement concerning the  $\langle \ln A \rangle$  behavior is also quite good when comparing with the CASA-MIA [8] and combined EAS-TOP and MACRO [9] measurements in which the analysis are performed in terms of a two mass groups (*light, heavy*) primary beam. Particularly significant is the comparison with the EAS-TOP and MACRO data, due to the much higher muon energy recorded in such experiment, showing that the obtained composition does not depend on the rapidity region of production of the secondaries.

### 3. References

1. Aglietta M. et al. (EAS-TOP Coll.), Nucl.Instr.Meth., A 336 (1993) 310.
2. Adinolfi Falcone R. et al. (EAS-TOP Coll.), Nucl.Instr.Meth., A 420 (1999) 117.
3. Alessandro B. et al. (EAS-TOP Coll.), Proc. 27th ICRC, Vol. 1, (2001) 124.
4. Kalmykov N.N., Ostapchenko S.S. and Pavlov A.J., Nucl. Phys. B 52 (1997) 17.
5. Heck D. and Knapp J., Extensive Air Shower Simulation with CORSIKA (5.61), Forschungszentrum Karlsruhe Report FZKA 6019 (1998).
6. Takahashi Y. et al. (JACEE Coll.), Nucler Physics B 60 (1998) 83.
7. Kampert K.-H. et al. (KASCADE Coll.) 27th ICRC, Invited, Rapporteur and Highlight Papers, (2001) 240.
8. Glasmacher M.A.K. et al. (CASA-MIA Coll.), Astrop. Phys., 12 (1999) 1.
9. Navarra G. et al. (EAS-TOP and MACRO Coll.), Proc. 27th ICRC, Vol. 1, (2001) 120.